RSC Advances

REVIEW

View Article Online
View Journal | View Issue

Cite this: *RSC Adv.*, 2022, **12**, 15447

Complete life of cobalt nanoparticles loaded into cross-linked organic polymers: a review

Muhammad Arif *

The unique combination of cobalt (Co) nanoparticles (NPs) and smart polymer microgels is of great interest and has received much attention over the past decade with respect to the production of hydrogen gas and its use in removing toxic dyes from water. The responsive behavior of microgels makes cobalt nanoparticle-loaded microgels most suitable for the production of hydrogen and for the reduction of pollutants in different environments. Different classes of Co NPs in microgels have been reported in the literature. Hybrid microgel formations play an important role in their use. Hence, a specific assembly of Co NPs in microgels has been designed for the synthesis and use of hydrogen to reduce toxic pollutants from water. All progress in the synthesis, classification, characterization, and applications of Co NPs in microgels has been reviewed in this report. Catalytic generation and the use of hydrogen for the reduction of pollutants in the presence of Co NPs loaded into microgels have been discussed in a tutorial manner.

Received 17th February 2022
Accepted 4th May 2022

DOI: 10.1039/d2ra01058e

rsc.li/rsc-advances

1. Introduction

Green fuel consumption is an important task nowadays.[1] All sources of consumption release heat along with toxic molecules into the environment, such as the burning of hydrocarbons that produces CO_2 and CO.[2] These produced gases are responsible for increasing the temperature of the environment and the deficiency of O_2 in the human body that ultimately leads to death. Green fuels such as H_2 gas are needed to avoid the creation of toxic environments.[3] The burning of H_2 gas produces energy along with water molecules. Water is essential for life. Thus, H_2 gas is the best green fuel for consumption purposes.[4] Hence, the production of hydrogen is very important due to its significant use. Generally, hydrogen gas is produced by catalysis.[5] Different materials are used for catalysis, such as metal–organic frameworks,[6] metal oxides,[7] and metal nanoparticles.[8] Nanoparticles are mostly used for the production of hydrogen, but the instability and cost of nanoparticles are the main issues facing their applicability. Stable metal nanoparticles are very costly but less stable nanoparticles are cheap. Co nanoparticles are of low cost and have catalytic activity comparable to that of noble metals for the catalytic production of hydrogen, but the instability of Co nanoparticles is their main drawback. This drawback can be diminished by using different stabilizers such as surfactants,[9] dendrimers,[10] micelles,[11] and microgels.[12] Microgels increase their stability as well as their catalytic performance to produce more hydrogen gas and are easily re-usable. Therefore, the best combination is that of cobalt nanoparticles with microgels. Microgels contain a cross-linked polymeric network in their structure. The microgels stabilize the metal nanoparticles due to the presence of electron donor sites in their structures.

This unique combination of metal nanoparticles and organic cross-linked polymeric network microgels has received great interest during the last few years because of its many applications in different fields such as medicine,[13] the purification of water,[14] and catalysis.[15] Hybrid microgels are mostly used for the catalytic generation of H_2 gas from $NaBH_4$ or NH_3BH_3 and then used to produce hydrogen for the reduction of toxic chemicals such as nitroarenes[16] and organic dyes[17] from

Department of Chemistry, School of Science, University of Management and Technology, Lahore 54770, Pakistan. E-mail: muhammadarif2861@yahoo.com; muhammadarif@umt.edu.pk

Muhammad Arif is a lecturer in Chemistry at the Department of Chemistry, School of Science, University of Management and Technology, Lahore, since 2017. He obtained his Ph.D in Chemistry from the Institute of Chemistry, University of the Punjab, Lahore, Pakistan. He obtained his M.Phil in Chemistry and M.Sc in Organic Chemistry from Quaid-i-Azam University Islamabad, Islamabad, and the Institute of Chemistry, University of the Punjab, Lahore, Pakistan. His research area is the synthesis, characterization and applications of metal nanoparticles fabricated in microgels.

water. Many review articles on different metal nanoparticle loaded microgels are reported in the literature[18–20] but cobalt nanoparticles loaded into microgels are not. Hence, it is a requirement for the new researchers to provide review articles on other metal nanoparticle loaded microgels due to suitable applications and cobalt nanoparticles loaded microgels are the most suitable combination for the generation of hydrogen and its use for the reduction of toxic materials. During the last decade, many researchers have researched on Co nanoparticle loaded microgels for catalytic production of hydrogen, reduction of nitroarenes, and organic dyes. Therefore, it is necessary to provide a review to the researchers, which works on generation of hydrogen and its use through catalysis in the presence of cobalt nanoparticles in microgels.

2. Classifications of Co nanoparticle loaded microgels

Cobalt NPs loaded in microgels are divided into different classes based on the morphology of hybrid microgels.

2.1 Microgel and metal nanoparticle-based hybrid microgels

Based on microgels and nanoparticles, hybrid microgels are divided into (i) monometallic (Co) nanoparticles loaded into homogeneous microgels[21–23] (ii) bimetallic nanoparticles loaded into homogeneous microgels[22] (iii) inorganic nanoparticles surrounded by cross-linked polymeric organic shell loaded with Co nanoparticles[23] (iv) Co nanoparticles loaded into porous microgels.

2.1.1 Monometallic (Co) nanoparticles loaded into homogenous microgel. Cobalt nanoparticles loaded into homogenous microgels have been mostly reported in the literature. In such types of cobalt nanoparticles into microgels, cross-linking density in hybrid microgels is the same in each part of the microgel and Co nanoparticles are introduced into the sieves of the polymeric network. Such type shows swelling and de-swelling behavior due to cross-linked polymeric network system at various stimuli. Ozay *et al.*[20] have synthesized Co, Ni, and Cu nanoparticles loaded into 2-acryl amido-2-methyl-1-propansulfonic acid (AAMPSA) microgel. They used these hybrid microgels for the generation of hydrogen gas by hydrolysis of ammonia borane (ABr) and sodium borohydride (NBH) and reported that more hydrogen gas was produced by NBH than ABr at the same time under similar conditions. Similarly, Seven and sahiner[22,23] have synthesized Co nanoparticles loaded into cross-linked organic polymeric microgels. They also reported the catalytic production of hydrogen gas. Hydrodynamic radius (Hdr) of hybrid microgels depends upon the concentration of the hydrophilic part. A large number of hydrophilic parts interact with more water molecules and show a large Hdr. A large number of salts are loaded by a more hydrophilic part and show better catalytic hydrogen production.

2.1.2 Bimetallic nanoparticles loaded into homogeneous microgels. Such systems of hybrid microgels are rarely reported. Mostly bimetallic nanoparticles loaded microgels have better results than monometallic with respect to catalytic as well as adsorption properties because both metals support each other to transport the electrons from the donor site to the acceptor in catalysis and in interactions with pollutants to remove them from water through adsorption. Ajmal *et al.*[22] have reported cobalt-nickel bimetallic nanoparticles loaded in poly(methacrylic-acrylonitrile) P(MA-AN) microgels. These bimetallic hybrid microgels were used for the adsorption study of different pollutants, such as dyes, toxic heavy metals, and herbicides, from water. Due to the paramagnetic behavior of these bimetallic nanoparticles, adsorbed toxic polluted materials were removed simply by applying magnetic fields along with a hybrid microgel. So, such systems are most suitable for reuse due to easy separation after the catalysis or adsorption process.

2.1.3 Inorganic nanoparticles surrounded by cross-linked polymeric organic shell loaded with Co nanoparticles. In such a core shell system, generally, the core is made up of silica or Fe_3O_4 or both and the shell with a cross-linked organic polymeric network. Nanoparticles are introduced into the shell of core shell microgels. Such a system is more suitable for catalysis because the substrate can easily reach the surface of nanoparticles through the cross-linked network, and the catalyst can be regained after catalysis by simply applying a magnetic field. Sahiner and Yasar[23] have synthesized silica and Fe_3O_4 containing core and cobalt nanoparticles loaded shell of poly(4-vinyl pyridine) P(4VP). These hybrid core shell microgels were used for catalysis to generate hydrogen gas from $NaBH_4$. The concentration of NaOH solution does not affect hydrogen production due to the acidic medium. NaOH solution can be used to prevent self-hydrolysis of SBH. Temperature increases the catalytic performance of such hybrid microgels by increasing the diffusion rate of SBH from the bulk region to the surface of cobalt nanoparticles and the number of collisions.

2.1.4 Cobalt nanoparticles loaded into porous microgels. In such types of microgels, the microgels are first prepared in a porous form, and then Co nanoparticles are introduced into the porous microgels. Nanoparticle loaded porous microgels have better catalytic results than homogenous hybrid microgels and core shell hybrid microgels. More nanoparticles are loaded in the porous microgel than in the bare microgel. So, the surface area of nanoparticles is increased in porous microgels due to the increased loading amount of the metal, and hence more active sites are present in porous hybrid microgels. Sahiner and Yasar[2626] have synthesized Co nanoparticles loaded into bare P(4VP) or P(4VP)-silica or porous P(4VP) separately. They used these synthesized hybrid microgels for the generation of hydrogen gas from $NaBH_4$ through catalytic hydrolysis. Cobalt nanoparticles loaded porous microgels showed better results in generating hydrogen (Table 1).

3. Synthesis of Co nanoparticle loaded microgels

The synthesis of cobalt nanoparticles loaded in microgels can be synthesized by mixing microgels and cobalt nanoparticles or microgels are synthesized first, followed by loading cobalt

Table 1 Classifications of cobalt nanoparticles loaded into microgels (representations of components: Co nanoparticles = dark red color, cross-linked organic polymer = dark blue)

Co NPs loaded into cross-linked polymer	Abbreviation of Co NPs loaded into polymer	Structure/morphology	Pictorial diagram	References
Monometallic (Co) nanoparticles loaded into homogenous microgel	Co NPs-AAMPSA	Monometallic homogenous structure	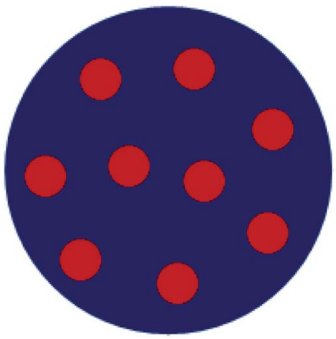	20
Bimetallic nanoparticles loaded into homogeneous microgels	Co–Fe NPs-P(MA-AN)	Bimetallic homogenous structure	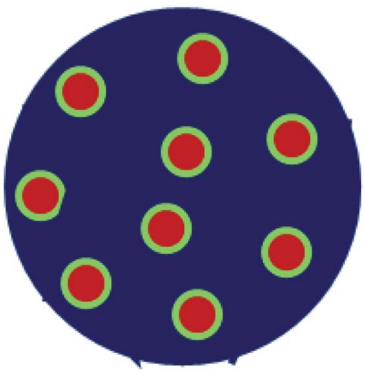	22
Inorganic nanoparticles surrounded by cross-linked polymeric organic shell loaded with Co nanoparticles	Fe_3O_4–SiO_2@Co NPs- P(4VP)	Core = Fe_3O_4–SiO_2 Shell = Co NPs loaded P(4VP)	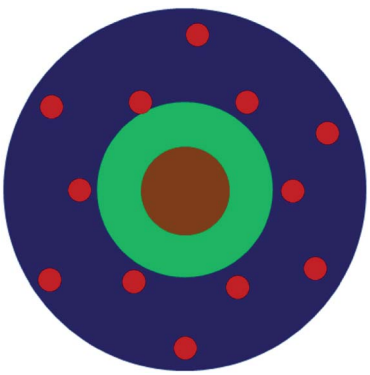	23
Cobalt nanoparticles loaded into porous microgels	Co NPs-P(4VP)	Porous hybrid microgels	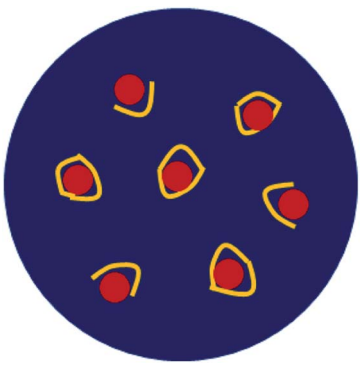	26

nanoparticles into microgels. Cross-linked polymeric networks can also be synthesized by different ways based on temperature and be given different names. If microgels are synthesized at low temperatures, then the microgels are called cryogels, and at higher temperatures (generally at 70 °C) called as microgels. The synthesis of hybrid microgels or hybrid cryogels is given below.

3.1 Synthesis of Co nanoparticles in microgel dispersion

In this process, microgel or cryogel is synthesized by adding the monomers along with a crosslinker and then adding the free radical initiator after maintaining the temperature at ≥70 °C under a nitrogen atmosphere. This is the free radical emulsion polymerization method (FREPM). Another method is the inverse suspension polymerization method (ISPM), in which both solvent and emulsifier are used during the synthesis of microgel.

In this method, one phase is aqueous, and the other is oil. Cobalt ions are introduced after the synthesis of the microgel in both ways and then reduced to form nanoparticles. Farooqi *et al.*[27] synthesized poly(*N*-isopropylacrylamide-*co*-methacrylic acid) (NipaM-*co*-MA) microgel by FREPM, as shown in Fig. 1. NipaM (monomer), MA (co-monomer), *N*,*N*-methylene bisacrylamide (bis) (crosslinker), and sodium dodecylsulphate (SDS) (stabilizer) were added into 95 mL de-ionized water in a three neck round bottom flask. Nitrogen purging was started along with the rising temperature with continuous stirring. 5 mL ammonium persulfate (APS) solution was added to the reaction mixture after maintaining the temperature at 70 °C. Reaction was continued for a further 4 h to obtain the microgel. Dialysis was done for 6 days to remove unreacted species from the mixture. Then, Co or Ni nanoparticles were introduced by reducing the respective salts.

Similarly, cryogels, which are basically microgels, have been synthesized at low temperatures. Sahiner and Yildiz[28] have synthesized cryogels by FRPM. 4VP, poly(ethylene glycol) diacrylate P(EGDA), and TemeD were added to water and cooled (T = 0 °C) for 5 min. KPS solution was added to polymerize and then transferred into a freezer with the help of plastic straws at −18 °C for 24 h. The obtained cryogels were washed with ethanol and water and then dried at 50 °C and stored in a desiccator. Then, ions were introduced and reduced into nanoparticles with the help of $NaBH_4$.

Rehman *et al.*[17] have synthesized poly(3-acrylamidopropyl)-trimethylammonium chloride P(AAPTMAC) microgel with ISPM. They optimized the condition for high yield synthesis of microgels by using different amounts of emulsifier and solvent to enhance the cross-linking density of the microgel. They added AAPTMAC monomer and bis crosslinker in an aqueous solution and then transferred this solution into a mixture of span 80 and gasoline at 800 rpm. *N*,*N*,*N*′,*N*′-

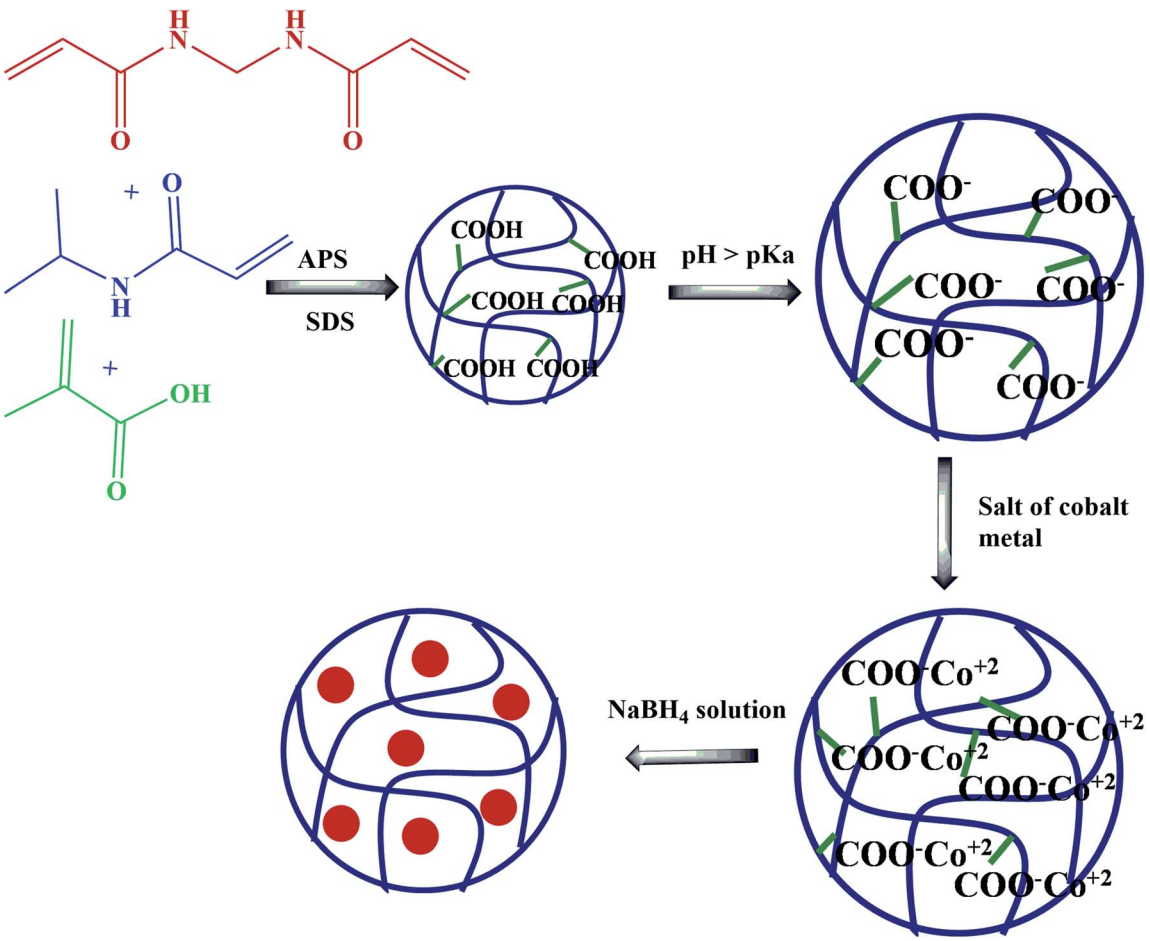

Fig. 1 Synthesis of poly(*N*-isopropylacrylamide-*co*-methacrylic acid) (NipaM-*co*-MA) microgels by the free radical polymerization method and the introduction of cobalt nanoparticles by *in situ* reduction.[27]

Tetramethylethylenediamine (TemeD) was added after 5 min. Then, APS solution was added after 15 min for polymerization. Polymerization was completed after 2 h. Synthesized microgel was poured into acetone solvent to remove impurities from the microgel. Then, cobalt, nickel, and copper solutions were prepared separately in ethanol. Then solution of metal salts is added into the microgel dispersion solution and reduced these salts into corresponding metal nanoparticles by *in situ* reduction with $NaBH_4$.

3.2 Synthesis of hybrid microgels by mixing nanoparticles and microgels

In this method, microgels and cobalt nanoparticles are synthesized separately and then mixed to produce cobalt nanoparticles loaded into microgels. The loading of nanoparticles into microgels is due to the electrostatic interaction that occurs between cobalt nanoparticles and microgels. Generally, microgels have electron donor sites, which interact with the nanoparticles, causing the loading into microgels. In this way, Chen *et al.*[29] have synthesized hybrid microgels, as shown in Fig. 2. They synthesized microgels by mixing NipaM, bis, and APS in deionized water in a vessel and sodium bisulphite (SBS) and a solution of NPs in another vessel. Both solutions were stirred for 30 min under a nitrogen atmosphere. Then, the first solution was poured into chlorobenzene (CB) and the other in *n*-hexane (NH). NH solution was added to the surface of CB. CB is denser than NH. So, the CB solution settles down, and NH is on the upper layer. The microgel and nanoparticles interact with each other due to electrostatic attraction at the interface region, forming hybrid microgels. Sidorov *et al.*[30] also synthesized hybrid microgels using the same method.

4. Characterization techniques used for microgels and hybrid microgels

Various techniques are used for the characterization of cobalt nanoparticles loaded in microgels. The reported techniques[31] for the identification of various parameters of hybrid microgels are summarized in Table 2.

The techniques used are; Transmission Electron microscopy (TEM), Scanning electron microscopy (SEM), X-ray diffraction (XRD), High Resolution Transmission Electron microscopy (HRTEM), Fourier Transformed Infrared Spectroscopy (FTIR), dynamic light scattering (DLS), energy dispersive X-rays (EDX), Thermo-gravimetric analysis (TGA), Atomic absorption spectroscopy (AAS), and UV/visible spectroscopy (UV-Vis).

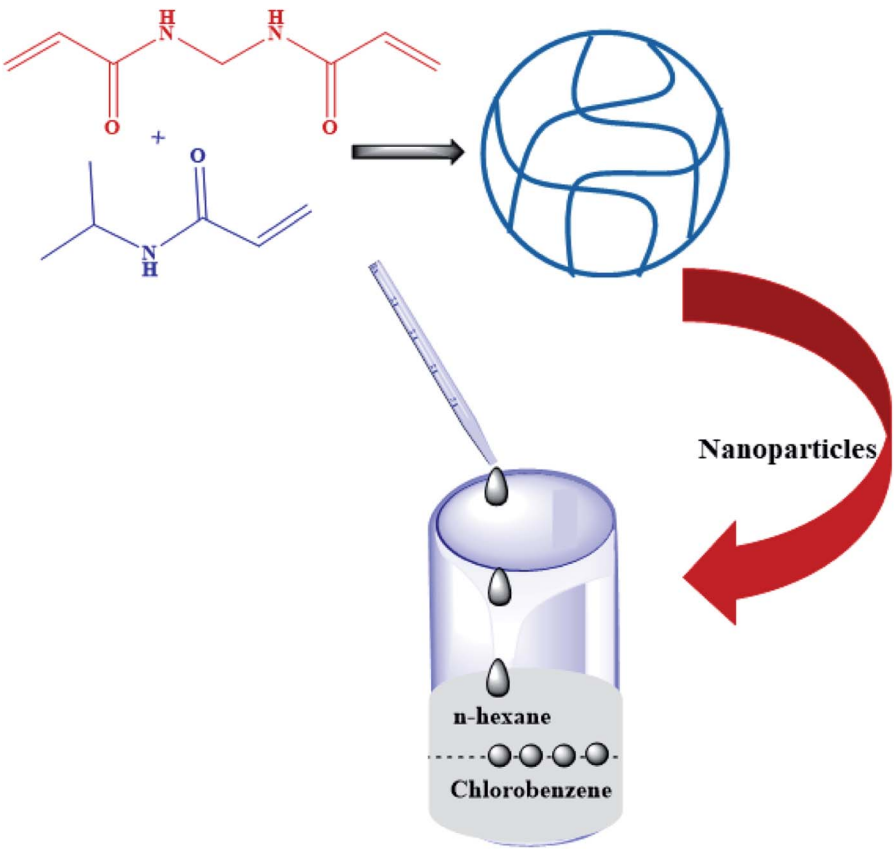

Fig. 2 Synthesis of the poly(*N*-isopropylacrylamide) P(NipaM) microgel and the hybrid microgel produced by mixing metal nanoparticles with the P(NipaM) microgel.[29]

Table 2 Summary of the characterization techniques used for the characterization of hybrid microgels and used of hybrid microgels for catalytic reactions

Co NPs loaded polymer	Used as catalyst	Characterization techniques	Identification by the techniques	Reference
Co NPs in P(VI) microgels (homogeneous hybrid microgel)	Generation of hydrogen by hydrolysis of $NaBH_4$	Zeta potential, FTIR, DLS, TGA, AAS, UV-Vis	Zeta-potential and DLS used to find the particle size, hydrodynamic radius, and surface charge. The size of P(VI)-por, P(VI), and P(VI)–Si microgels were 764 nm, 304 nm, and 530 nm, respectively, according to DLS technique. Hdr of P(VI)-por was greater than P(VI)–Si due to generation of pores after the removal of Si and more water intake. The zeta-potential value of P(VI)-por, P(VI), and P(VI)–Si microgels were −21.99 mV, 1.20 mV, and −19.86 mV, respectively. A more negative value of P(VI)-por microgel indicates that some amount of Si is present in the microgel in porous form. Different functionalities from microgel characterized with the help of FTIR. P(VI) microgels lost 90% weight, and weight-loss of P(VI)-por and P(VI)–Si were almost similar (31.3% wt and 34.4% wt, respectively), which was indicated by the TGA technique. The contents of Co nanoparticles in P(VI), P(VI)-por, and P(VI)–Si microgels were 7.71, 8.56, and 8.46, respectively, calculated with AAS	26
Co NPs loaded in P(4VP) cryogel (homogeneous hybrid microgel)	Hydrogen generation by hydrolysis of $NaBH_4$ and NH_3BH_3	FTIR, TGA, AAS	FTIR technique was used to identify the presence of different functional groups present in microgels and hybrid microgels. The content of Co nanoparticles in Co NPs loaded P(4VP) microgel was 11.5 wt%, which was found with the help of TGA in the first loading. This amount was increased by increasing the loading steps. This amount was 25.4 wt% in the third and 33 wt% in the fifth loading. The contents of Co NPs according to the AAS technique were 20.49, 49.97, 85.4, 94.5, and 97.3 mg g^{-1} in 1^{st}, 2^{nd}, 3^{rd}, 4^{th}, and 5^{th}	28

Table 2 (*Contd.*)

Co NPs loaded polymer	Used as catalyst	Characterization techniques	Identification by the techniques	Reference
			loading. In continuously loading the metal, the metal content increases and hence the active sites for catalytic performance	
Metal NPs in P(NipaM)/P(HemA) (homogeneous hybrid microgel)	Can be used for catalysis	^{1}H NMR, TEM, FTIR, EDS, SEM, UV-Vis	The structure of the microgel has been characterized by ^{1}H NMR. Functionalities of microgel and hybrid microgel identified with FTIR. Size of the microgel identified with SEM and metal nanoparticles with TEM techniques. The diameter of microgels was from 150 to 1000 μm and metal nanoparticles from 5 to 6 nm for Au, 20–25 for Ag and 30 for Co nanoparticles loading in microgels	29
Co NPs loaded into poly(ethylene imine) P(EI) (homogeneous hybrid microgel)	Generation of H_2 by hydrolysis of $NaBH_4$ and catalytic reduction of 4-nitrophenol	SEM, FTIR, TGA, DLS, zeta potential	SEM technique was used to determine the spherical morphology and size of the microgel in the swollen state. The particle size of microgels was in the range of 10 nm to 10 μm. Different functionalities of polymer particles and microgels were confirmed by FTIR. Property of thermal stability of polymer particle and microgels characterized with TGA technique. TGA indicated that the stability of the microgel is slightly more than the hybrid. The difference of wt% between polymer and microgels is 17.44%, which is the cross-linking density value. The size in diameter of microgel, obtained by zeta potential, without and with filtration were 1175 and 558 nm, respectively	32
Co NPs onto porous P(4VP) microgel (porous hybrid microgel)	Generation of H_2 by hydrolysis of $NaBH_4$	DLS, zeta potential, FTIR, AAS, BET	FTIR technique has been used to identify different functionalities and incorporation of nanoparticles in the porous surface due to the shifting of stretching frequency. Particle sizes were 333, 398, and 478 nm for P(4VP), P(4VP)-silica, and P(4VP)-porous microgels, respectively, which were obtained by the DLS	25

Table 2 (*Contd.*)

Co NPs loaded polymer	Used as catalyst	Characterization techniques	Identification by the techniques	Reference
			technique. Surface areas of these microgels obtained with the help of the BET technique were 43.78, 24.02, and 42.26 $m^2 g^{-1}$ for P(4VP)-silica, P(4VP), and P(4VP)-porous, respectively. TGA has been used to check the stability of microgels. P(4VP) lost 15.5% more amount as compared to P(4VP)-silica	

5. Applications of cobalt nanoparticles into microgels

5.1 Cobalt nanoparticle loaded microgels for hydrogen production

Different sources for the production of hydrogen gas have been reported in the literature[33–36] but here, our main concern is the synthesis of hydrogen gas by cobalt nanoparticles loaded into microgels. According to my best effort of the literature survey, only ammonia borane and $NaBH_4$ (substrates) are reported for hydrogen gas generation by Co NPs loaded into microgels. Ozay *et al.*[20] synthesized cobalt, nickel, and copper NPs loaded microgels separately and reported that the catalytic activity of cobalt NPs loaded microgel was more than that of nickel or copper nanoparticle loaded microgels. 186 ml of hydrogen gas was produced in 25 min, 65 min, and 75 min by Co, Cu, and Ni NPs loaded microgel using ammonia borane. This catalytic performance may be due to a large amount of Co NPs than other NPs in the microgel because of more active sites. Seven and Sahiner[21] reported the comparative study of $NaBH_4$ and NH_3BH_3. They reported that NH_3BH_3 is a better source for hydrogen production than $NaBH_4$ in a basic medium.

5.1.1 Factors affecting hydrogen gas generation by Co NPs in microgels. Different factors affect the catalytic performance of cobalt nanoparticles loaded into microgels in the production of hydrogen gas. Here, we will discuss these factors one by one.

5.1.1.1 Effect of temperature. The temperature has an important role in the generation rate of hydrogen gas by hybrid microgels and substrates. The kinetic energy of molecules is increased by increasing the temperature, and the kinetic energy of molecules is directly proportional to the number of collisions of hybrid microgels and the substrate. According to collision theory, when the number of collisions is increased, then the rate of product formation is also increased.

On the other hand, the diffusion rate of the substrate is also increased from the bulk region to the surface of nanoparticles. It means that when the temperature is increased, the rate of hydrogen gas production also increases, and the reaction occurs in a short time, as shown in Fig. 3. Sahiner and Yildiz[28] have reported that cobalt NPs in P(4VP) produced hydrogen gas at a higher rate at high temperatures. Here, they did not study the generation of hydrogen at 0 °C. Turhan *et al.*[35] studied the production of hydrogen gas at 0 °C. They indicated that the production of hydrogen gas may be applicable at low temperature as well as high temperature, but the rate of reaction increases continuously by increasing the temperature.

5.1.1.2 pH effect. The pH of a solution also affects the production rate of hydrogen gas by affecting the structure of

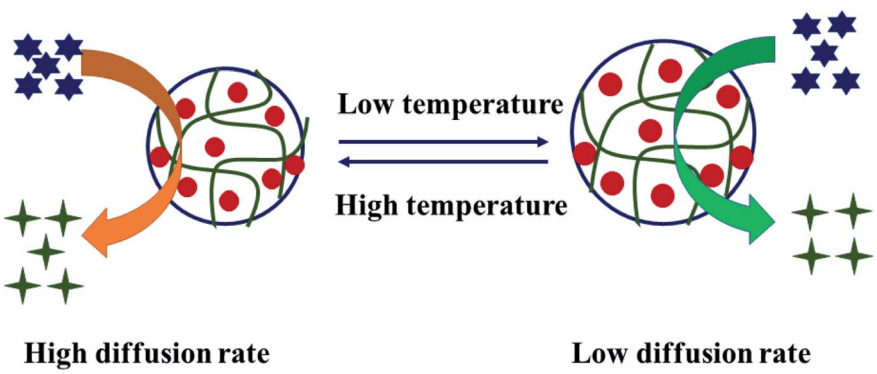

Fig. 3 Production of hydrogen at low and high temperatures in the presence of Co nanoparticles in P(4VP) microgels.[28]

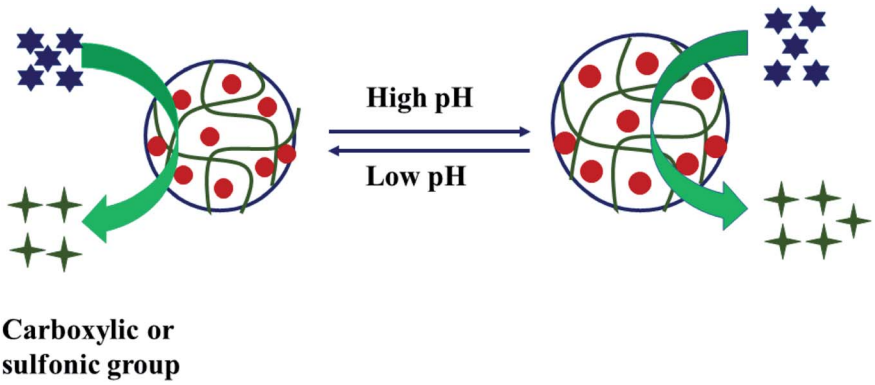

Fig. 4 Effect of pH on the –COOH or $–SO_3H$ group-containing hybrid microgels (acidic group-containing hybrid microgels).[24]

hybrid microgels. The polar part of hybrid microgels have –COOH, $–SO_3H$, and –NH– or –N═ groups in their structure. –COOH and $–SO_3H$ are acidic groups and can donate protons in water. In the deprotonated form, they have a negative charge, and due to the same charge, electrostatic repulsion occurs, and microgel swells. In the swollen state, a greater number of nanoparticles are loaded into microgels. So, such hybrid microgels show a higher rate at higher pH and a lower rate at a lower pH value of the medium, as shown in Fig. 4. On the other hand, in the swollen state, the substrate can easily reach the surface of nanoparticles, easily producing hydrogen gas. In the charged form, the hybrid microgel strongly interacts with water molecules, and water diffuses into the hybrid microgels. BH_4^- ions also easily diffuse and reach the surface of nanoparticles, and hence the rate of generation is also increased. On the other hand, the amino group is basic in nature, and it can accept protons. This group has a positive charge in the protonated form. Due to electrostatic repulsion, the Hdr of microgels increases, and a greater number of nanoparticles can be introduced into microgels. Their hydrogen gas production rate from substrate also increases due to the presence of more active sites of nanoparticles, as shown in Fig. 5. In this way, pH can affect the production rate of hydrogen gas by changing the protonated or deprotonated form of hybrid microgels.

Sahiner and Yasar[36] have synthesized hybrid microgels using P(2VP) microgels and both P(2VP-*co*-4VP) microgels. More hydrogen production rate was observed at low pH due to protonation of amino groups. They also reported that the catalytic performance of hybrid microgels was increased by increasing the amount of 4VP as compared to 2VP. In 4VP, the nitrogen atom is away from the electron donating vinyl group, and hence it can easily interact with the ions without competition. So, more nanoparticles are loaded in microgels, and catalytic activity is also increased. Seven and Sahiner[24] have synthesized nanoparticle loaded P(Am-Vsa) microgels. They also reported the same behavior by increasing the Vsa concentration, and the production rate was calculated at high pH due to swollen state.

5.1.1.3 Effect of cobalt NPs on microgels, macrogels, and cryogels. Basically, the rate of hydrogen gas generation is controlled by controlling the size of NPs and cross-linking area or the area of sieves and temperature. Cross-linking density is inversely proportional to the area of sieves. The size of nanoparticles can be controlled by controlling the area of sieves. If the area of sieves is small, then small sized nanoparticles are produced, which have more surface area. So, the rate of hydrogen production is increased. The area of sieves is greater in macrogels than in microgels. So, the catalytic activity for hydrogen production is more by hybrid microgels than hybrid macrogels. The catalytic performance of hybrid microgels is greater than hybrid cryogels because hybrid microgels uptake more water than hybrid cryogels. So, the Hdr of hybrid microgel is greater than hybrid cryogels.[37] Hybrid cryogels are produced at low temperatures, usually 0 °C. So, the coagulation of

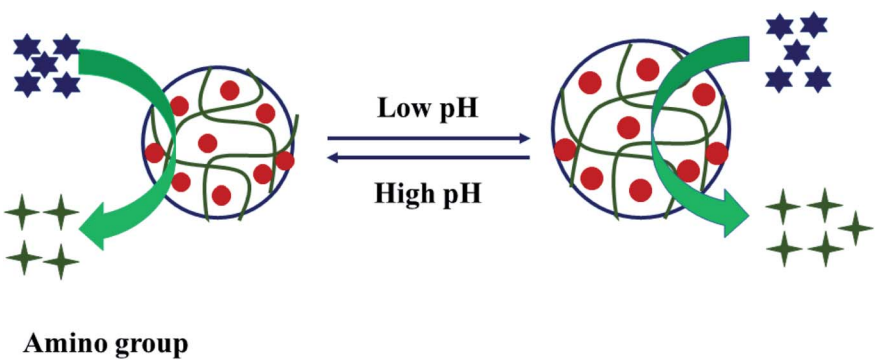

Fig. 5 Effect of pH on amino group-containing hybrid microgels (basic group-containing hybrid microgels).[36]

nanoparticles can be controlled at 0 °C. Turhan *et al.*[35] have synthesized 3-sulfopropyl methacrylate (3SPM) in micro and macrogel form with and without a stabilizer. Co and Ni NPs were introduced by *in situ* reduction. The rate of hydrogen production of hybrid microgels was greater than that of hybrid macrogels. Co NP-loaded P(3SPM)-micro and P(3SPM)-macrogels produced 248 ml hydrogen gas in 15 min and 26 min, respectively. Similarly, Sahiner and Demirci[38] also reported the order of catalytic performance of cobalt NPs in micro-, macro-, and cryogels for hydrogen generation. Hybrid microgels showed better results than cryogels, followed by macrogels. 154 ml of hydrogen gas was produced by hybrid micro-, macro-, and cryogels in 55 min, 105 min, and 85 min, respectively.

5.1.1.4 Solvent effect. Solvents also play an important role in hydrogen gas generation. The solvent is the medium, which supports the substrate to reach the surface of nanoparticles. It also interacts with the substrate and hybrid microgels. If the interaction of the substrate or hybrid microgel is more with the solvent than between substrates and hybrid microgels, then the substrate reaches slowly on the surface of nanoparticles, and hence the rate of hydrogen generation becomes low. Sahiner *et al.*[39] have used cobalt nanoparticle based P(4VP) microgels to generate hydrogen gas in aqueous and methanol solvents. 250 ml hydrogen gas is produced by methanolysis of $NaBH_4$ in 5 min in the presence of cobalt nanoparticle composite with P(4VP) microgels, which is more than in water solvent. The oxygen atom is an inferior electron donor in methanol than in water. The solvent, which facilitates to donate the electrons, show a better result for catalytic hydrogen gas production. Another reason is the higher protonation of nitrogen atoms by methanol as compared to water, which is present in hybrid microgels. Due to this protonation, more electrostatic attraction is generated. Borohydride ions interact strongly with hybrid microgels and hence reach the surface of Co nanoparticles in microgels. Yildiz *et al.*[40] have reported the hydrogen gas generation in deionized water, tap water, and seawater and reported that hydrogen gas is produced more rapidly in seawater than in tap water and then deionized water. More H_2 gas is produced in seawater due to the effect of ions. Khan *et al.*[41] also reported the studies in methanol solvent.

5.1.1.5 Effect of hydrophilic part of hybrid microgels. The hydrophilic part of hybrid microgels has an important role in hydrogen production by the substrate. The hydrophilic part contains partial positive and partial negative charges on hybrid microgels. These partial charges have the capacity to interact with ions or water or polar species. Due to stronger interaction with water, the hydrodynamic radius (Hdr) of microgels has been increased, and a large amount of metal ions can be loaded into the cross-linked polymeric structure of microgels. These ions are converted into NPs by reduction. In this way, more nanoparticles are introduced into the microgels. More nanoparticles mean more active sites and hence a more rapid hydrogen production rate. On the other hand, the hydrophilic part interacts with hydrides with more electrostatic force, and hence the substrate can easily reach the surface of nanoparticles. Seven and Sahiner[24] have synthesized cobalt and nickel nanoparticles loaded poly(acrylamide-*co*-vinyl sulfonic acid) P(Am-Vsa) microgels separately. They reported that if the amount of Vsa is more in microgels, then a greater number of nanoparticles are introduced into it. They used 1.5 : 1, 1 : 1, and 1 : 1.5 ratios of Am and Vsa for the synthesis and used their hybrid microgels for hydrogen production by $NaBH_4$ in an aqueous medium. The rate of hydrogen gas production was more in which the ratio of Am and Vsa was 1 : 1.5. Similar behavior was reported by Sahiner and Yasar.[36]

5.1.1.6 Salt effect. Salts also affect the H_2 production rate. Salts prevent $NaBO_4$ accumulation on the surface of nanoparticles. $NaBO_4$ occupies the active sites of nanoparticles by accumulation. Therefore, it is essential to remove it from the surface of nanoparticles, and salts can do so, as shown in Fig. 6. So, salts increase the rate of hydrogen production. Ionic strength and size of ions can control the removal of $NaBO_4$ from the nanoparticle surface. So, when the ionic strength is more, it interacts with more power to BO_4^- ions than others. Similarly, if the size of the ion is small, then it will interact with more power.

Yildiz *et al.*[40] have synthesized metal NPs embedded P(3SPM) microgels. They studied the effect of ionic solutions on hydrogen

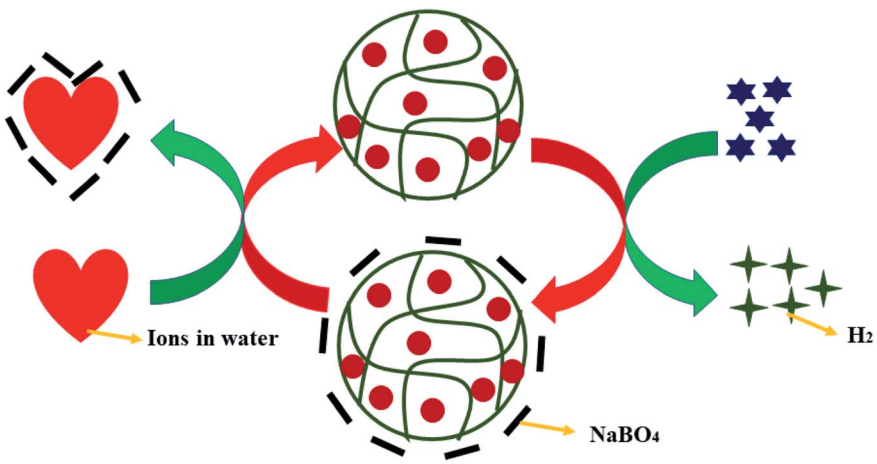

Fig. 6 Effect of salts on the catalytic performance of cobalt nanoparticles loaded into P(3SPM) microgels.[40]

generation. They used NaCl, KCl, and $CaCl_2$ salts. The rate of hydrogen generation was NaCl > $CaCl_2$ > KCl. Na^+ ions have a smaller size as compared to K^+ ions. So, Na^+ ions interact more strongly with BO_4^- ions than K^+ ions. Ca^{2+} ions have more ionic strength, but sulphonic groups interact more strongly than BO_4^- ions. So, Na^+ ions interact more strongly with BO_4^- ions, and hence the production rate was high in the presence of NaCl.

5.2 Uses of produced hydrogen gas in the presence of cobalt nanoparticle loaded microgels

Hydrogen gas has various applications but its production by cobalt nanoparticle composites with microgels is rare. Mostly hydrogen, which is produced by Co NPs loaded into microgels and $NaBH_4$ or NH_3BH_3 is used to remove toxic chemicals such as nitroarenes and organic dyes.[16,42]

5.2.1 Catalytic reduction of nitroarenes. Nitroarenes are toxic chemicals present in water. They are converted into less toxic aminoarenes in the presence of cobalt nanoparticles in microgels. During the reduction of nitroarenes, Co nanoparticles first converted $NaBH_4$ or NH_3BH_3 into hydrogen gas and boron oxide, and hydrogen reacts with nitroarenes to form aminoarenes. Demirci *et al.*[43] synthesized and used a hybrid microgel to generate first hydrogen gas and then used the produced hydrogen gas for reduction of 4NP. One of us has extracted Co^{2+} ions from water by microgels and then reduced Co^{2+} ions into Co nanoparticles and used them for the reduction of 4NP (4-nitrophenol).[15] Reduction of nitroarenes depends upon different factors, such as if the reduction of nitroarenes is performed in deionized water, tap water, and dam water, then the reduction rate is different due to the presence of different types of interactions. Those with more interaction with nanoparticles are attached to it first. The reduction of nitroarenes performed in deionized water shows a faster reduction rate than in tap and dam water. Tap and dam water contain impurities that interfere during the interaction of the substrate with cobalt nanoparticles. So, more impurities mean more interference. Dam water contains more impurities. Therefore, the reduction rate was minimum in dam water and maximum in deionized water. Naeem *et al.*[42] have synthesized Co nanoparticles loaded into methacrylic acid microgel and reported a similar behavior for reduction of 4-nitroarenes in tap, deionized, and dam water.

The temperature factor also controls the reduction rate of nitroarenes. Generally, the reduction rate of nitroarenes increases as the temperature increases because the diffusion rate of the substrate also increases from the bulk region to the surface of nanoparticles. As temperature increases, the collision number is also increased. So, the reduction rate increases along with the temperature. Sahiner and Demirci[44] synthesized Co nanoparticle loaded (4VP) microgel and used it for the reduction of 4NP at various temperatures. The reduction rates of 4NP at 10, 20, 30, 40, and 50 °C were 0.0008, 0.0013, 0.0017, 0.0021, and 0.0023 s^{-1}, respectively. This result showed that the reduction rate is increased with increasing temperature due to the high diffusion rate at high temperatures. Demirci and Sahiner also reported the same behavior for the reduction of 4NP and 2NP at different temperatures.

The pH of the medium also controls the rate of reduction of nitroarenes. The hybrid microgels, which have –COOH or $–SO_3H$ groups in their structure, rapidly increase their Hdr by increasing the pH value greater than the pK_a value. This happens due to the electrostatic repulsion of anions ($–COO^-$, $–SO_3^-$) of hybrid microgels, and under this condition, the substrate can easily diffuse from bulk to the surface of nanoparticles and then from the surface to bulk after conversion into the product. In this way, we can say that these hybrid microgels show better reduction performance in the basic medium. On the other hand, those hybrid microgels, which have an amino group in their structure, have high Hdr at low pH due to electrostatic repulsion between the same charges. Farooqi *et al.*[27] studied the effect on Hdr of hybrid microgel and reported that

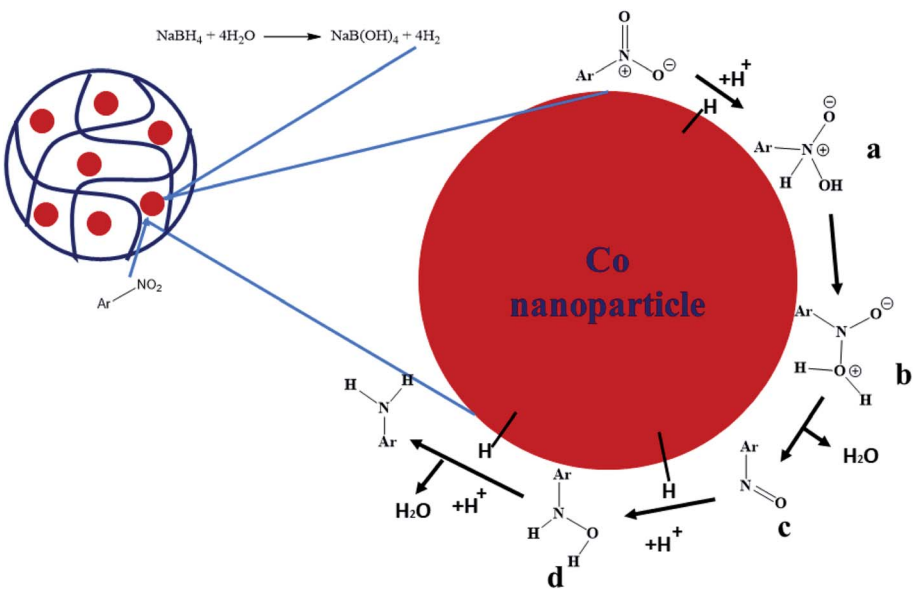

Fig. 7 Proposed mechanism for the reduction of nitroarenes in the presence of Co NPs loaded into microgels.[16,45]

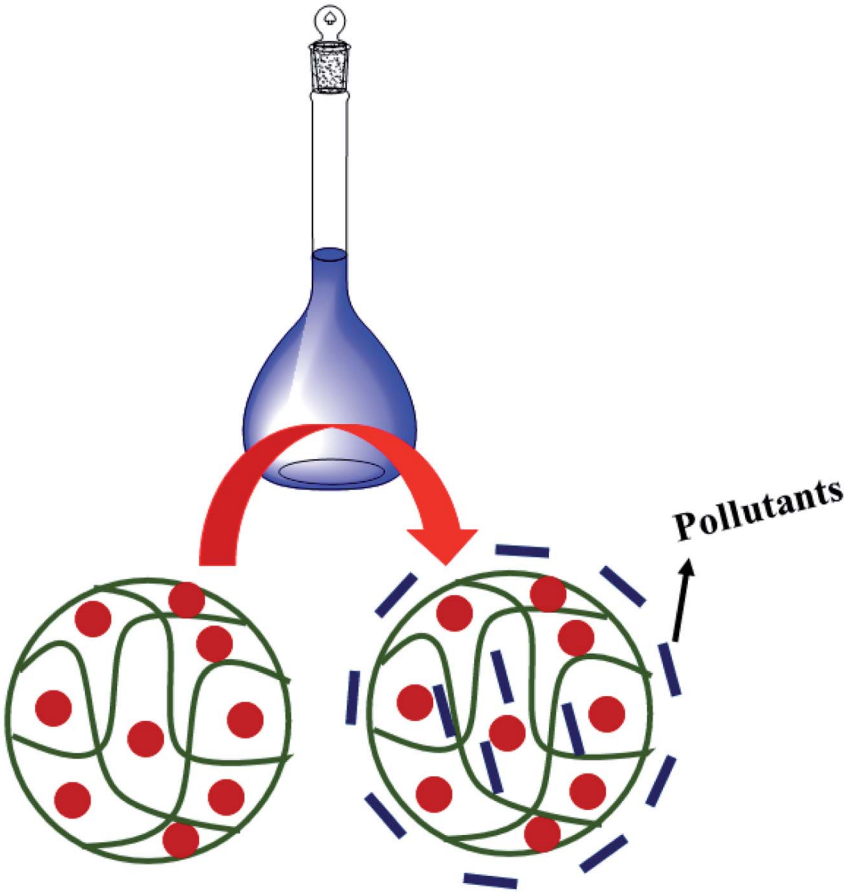

Fig. 8 Adsorption process of Co–Fe nanoparticles loaded into P(MA-AN) microgels.[22]

at pH > pK_a have a greater Hdr of hybrid microgels. They did not study the effect on catalytic behavior.

Catalytic reduction of nitroarenes consists of different steps as shown from a to d in Fig. 7.[16,45] In the first step, a proton from water and hydride from BH_4^- attach with the nitro group of nitroarenes to form a. Then, rearrangement takes place to form b. In the next step, the water molecule detaches from the nitroso group to form **c**. Hydride and proton are attached to the nitroso group to form **d**. In the last, the **d** form is converted into an amino group, which detached from the surface of cobalt nanoparticles. The surface of cobalt nanoparticles provides a field to transport the electrons from borohydride to electron deficient nitroarenes and reduce this nitro group from nitroarenes.

5.2.2 Catalytic reduction of organic dyes. The produced hydrogen can be used to reduce toxic organic dyes from water. The reduction rate of dyes in the presence of cobalt nanoparticle loaded microgels depends upon the nature of the dye and microgel. Those hybrid microgels, which have –COOH and –SO_3H groups in their structure, reduced cationic dyes more rapidly as compared to neutral or anionic dyes in a basic medium. Electrostatic attraction is responsible for better catalytic performance. Similarly, –NH_2 group containing hybrid microgels show better performance at low pH with anionic dyes as compared to cationic and neutral dyes. The electrostatic attraction facilitates the substrate to reach the surface of nanoparticles and easily approach the substrate on the surface, increasing the rate of reduction. Farooq *et al.*[46] have synthesized hybrid microgels and used them for the reduction of methyl orange (MO), 2NP, and NP. Similarly, Ajmal *et al.*[14,47] have synthesized hybrid microgels to reduce MO, EY, 2NP, 4NA, and 4NP. The reduction order of the compounds is as follows: 4NP > 2NP > 4NA > MO. The reduction rate of 4NP is the greatest among these because of its higher polarity than others. MO has the least reduction rate due to less interaction with hybrid microgels.

5.3 Adsorption of pollutants

Cobalt nanoparticle loaded microgels can be used as adsorbents to remove toxic chemicals such as metal ions, organic dyes, and herbicides from water. Hybrid microgels have polar parts in their structures. These polar parts interact with these toxic chemicals from water due to electrostatic interactions, as shown in Fig. 8. When toxic chemicals are attached to hybrid microgels, they can be removed by applying magnetic fields for ferronematic materials or centrifugation. Ajmal *et al.*[22] have synthesized cobalt and iron nanoparticles in microgels and used them for the removal of Cd^{2+} ions, Cr^{3+} ions, paraquats (PQ), herbicides, Rh–B, and MB from water by adsorption process and separated simply by applying a magnetic field. They

also reported that the adsorption property of hybrid microgels was increased by increasing the polarity (converting the nitrile group into an amidoxime group). The adsorption capacity increased from 56.3, 57.4, 75.3, 37.4, and 40.2 to 166.5, 334.5, 190.0, 89.9, and 88.1 for Cr^{3+}, Cd^{2+}, PQ, Rh–B, and MB respectively. Similarly, Bibi *et al.*[48] have also used microgels and hybrid microgels to remove MB through the adsorption process.

6. Conclusions and future directions

The aim of this review article was to report the current research developments in the design, stabilization, and fabrication of cobalt nanoparticles loaded in microgels and the use of these cobalt nanoparticle loaded microgels for more hydrogen gas generation to adopt the most suitable condition. The suitable conditions for the generation of hydrogen gas were discussed in detail. This produced hydrogen gas was used to remove toxic chemicals such as nitroarenes and organic dyes from an aqueous medium. The catalytic reduction of nitroarenes and organic dyes can easily be monitored with a UV/visible spectrophotometer. Cobalt nanoparticle loaded microgels have a unique combination, which can remove toxic chemicals such as heavy metals ions, dyes, herbicides, paraquats, and nitroarenes by catalysis as well as adsorption process.[15–24] Only ammonia borane and $NaBH_4$ were used for hydrogen gas generation. Other substrates like water can also be studied in the future. Different morphologies of hybrid microgels for catalytic hydrogen generation and reduction of dyes are important topics for future studies. The monomers and co-monomers of microgels reported in the literature are non-biodegradable materials. They can be replaced by biodegradable materials such as 4-vinylcaprolactam in future studies. In the catalytic reduction of nitroarenes, mostly, 4NP is used as a model reaction. Catalytic reduction of a limited number of dyes by cobalt nanoparticle loaded microgels has been reported in the literature. Cobalt nanoparticle loaded microgels can be used for catalytic reduction of toxic metal ions such as Cr^{6+}, Hg^{2+}, Cd^{2+}, *etc.*, in the future.

Conflicts of interest

There is no conflict of interest.

List of abbreviations

NPs	Nanoparticles
AAMPSA	2-Acryl amido-2-methyl-1-propansulfonic acid
ABr	Ammonia borane
4AP	4-Aminophenol
NBH	Sodium borohydride
Hdr	Hydrodynamic radius
MA	Methacrylic
AN	Acrylonitrile
4VP	4-Vinyl pyridine
DLS	Dynamic light scattering
FREPM	Free radical emulsion polymerization method
ISPM	Inverse suspension polymerization method
EDX	Energy dispersive X-rays
FTIR	Fourier Transform Infrared Spectroscopy
NipaM	*N*-Isopropylacrylamide
HRTEM	High resolution transmission electron microscopy
LCST	Lower critical solution temperature
SDS	Sodium dodecylsulphate
bis	*N*,*N*-Methylene bisacrylamide
APS	Ammonium persulfate
P(EGDA)	Poly(ethylene glycol) diacrylate
P(AAPTMAC)	Poly(3-acrylamidopropyl)-trimethylammonium chloride
TemeD	*N*,*N*,*N*′,*N*′-Tetramethylethylenediamine
SBS	Sodium bisulphite
CB	Chlorobenzene
NH	*n*-Hexane
PnvcL	Poly(*N*-vinylcaprolactam)
SEM	Scanning electron microscopy
TGA	Thermo gravimetric analysis
AAS	Atomic absorption spectroscopy
3SPM	3-Sulfopropyl methacrylate
Vsa	Vinyl sulfonic acid
Am	Acrylamide
UV-Vis	UV/visible spectroscopy
VPTT	Volume phase transition temperature
XPS	X-ray photoelectron spectroscopy
XRD	X-ray diffraction
MO	Methyl orange

Acknowledgements

Muhammad Arif is thankful to the University of Management and Technology, Lahore for providing the facility to carry out a part of work.

References

1 K. Karagul, Y. Sahin, E. Aydemir and A. Oral, in *Lean and green supply chain management*, Springer, 2019, pp. 161–187.
2 P. Chiesa, S. Consonni, T. Kreutz and R. Williams, *Int. J. Hydrogen Energy*, 2005, **30**, 747–767.
3 A. S. A. A. Hamaad, M. Tawfik, S. Khattab and A. Newir, *Procedia Environ. Sci.*, 2017, **37**, 564–571.
4 A. Demirbas, *Energy Resources*, 2017, **24**, 601–610.
5 S. Demirci and N. Sahiner, *Fuel Process. Technol.*, 2014, **127**, 88–96.
6 X. Wang, J. He, B. Yu, B. Sun, D. Yang, X. Zhang, Q. Zhang, W. Zhang, L. Gu and Y. Chen, *Appl. Catal., B*, 2019, **258**, 117996.
7 Y. Kojima, K. I. Suzuki, K. Fukumoto, M. Sasaki, T. Yamamoto, Y. Kawai and H. Hayashi, *Int. J. Hydrogen Energy*, 2002, **27**, 1029–1034.
8 C. E. Bunker and M. J. Smith, *J. Mater. Chem.*, 2011, **21**, 12173–12180.
9 Y. Bao, W. An, C. H. Turner and K. M. Krishnan, *Langmuir*, 2009, **26**, 478–483.

10 K. Aranishi, Q.-L. Zhu and Q. Xu, *ChemCatChem*, 2014, **6**, 1375–1379.
11 O. A. Platonova, L. M. Bronstein, S. P. Solodovnikov, I. M. Yanovskaya, E. S. Obolonkova, P. M. Valetsky, E. Wenz and M. Antonietti, *Colloid Polym. Sci.*, 1997, **275**, 426–431.
12 A. Biffis, N. Orlandi and B. Corain, *Adv. Mater.*, 2003, **15**, 1551–1555.
13 J. Ihsan, M. Farooq, M. A. Khan, M. Ghani, L. A. Shah, S. Saeed and M. Siddiq, *Microsc. Res. Tech.*, 2021, **84**, 1673–1684.
14 M. Ajmal, S. Demirci, M. Siddiq, N. Aktas and N. Sahiner, *New J. Chem.*, 2016, **40**, 1485–1496.
15 M. Shahid, Z. H. Farooqi, R. Begum, M. Arif, A. Irfan and M. Azam, *Chem. Phys. Lett.*, 2020, **754**, 137645.
16 N. Jabeen, Z. H. Farooqi, A. Shah, A. Ali, M. Khurram, K. Mahmood, N. Sahiner and M. Ajmal, *J. Porous Mater.*, 2021, **2021**(1), 1–14.
17 S. Rehman, M. Siddiq, H. Al-Lohedan and N. Sahiner, *Chem. Eng. J.*, 2015, **265**, 201–209.
18 M. Arif, Z. H. Farooqi, A. Irfan and R. Begum, *J. Mol. Liq.*, 2021, **336**, 116270.
19 R. Begum, K. Naseem and Z. H. Farooqi, *J. Sol-Gel Sci. Technol.*, 2016, **77**, 497–515.
20 O. Ozay, E. Inger, N. Aktas and N. Sahiner, *Int. J. Hydrogen Energy*, 2011, **36**, 8209–8216.
21 F. Seven and N. Sahiner, *Int. J. Hydrogen Energy*, 2013, **38**, 15275–15284.
22 M. Ajmal, M. Siddiq, N. Aktas and N. Sahiner, *RSC Adv.*, 2015, **5**, 43873–43884.
23 N. Sahiner and A. O. Yasar, *Fuel Process. Technol.*, 2016, **144**, 124–131.
24 F. Seven and N. Sahiner, *Int. J. Hydrogen Energy*, 2013, **38**, 777–784.
25 N. Sahiner and A. O. Yasar, *Int. J. Hydrogen Energy*, 2013, **38**, 6736–6743.
26 N. Sahiner and A. O. Yasar, *Fuel Process. Technol.*, 2013, **111**, 14–21.
27 Z. H. Farooqi, S. Iqbal, S. R. Khan, F. Kanwal and R. Begum, *e-Polymers*, 2014, **14**, 313–321.
28 N. Sahiner and S. Yildiz, *Fuel Process. Technol.*, 2014, **126**, 324–331.
29 Z. Chen, L. Hu and M. J. Serpe, *J. Mater. Chem.*, 2012, **22**, 20998–21002.
30 S. N. Sidorov, L. M. Bronstein, V. A. Davankov, M. P. Tsyurupa, S. P. Solodovnikov, P. M. Valetsky, E. A. W. and R. J. Spontak, *Chem. Mater.*, 1999, **11**, 3210–3215.
31 H. Park, L. Srisombat, A. Jamison, T. Liu, M. Marquez, H. Park, S. Lee, T.-C. Lee and T. Lee, *Gels*, 2018, **4**, 28.
32 N. Sahiner, *Colloids Surf., A*, 2013, **433**, 212–218.
33 D. S. A. Simakov and M. Sheintuch, *AIChE J.*, 2011, **57**, 525–541.
34 L. Shi, Z. Chen, Z. Jian, F. Guo and C. Gao, *Int. J. Hydrogen Energy*, 2019, **44**, 19868–19877.
35 T. Turhan, Y. A. Güvenilir and N. Sahiner, *Energy*, 2013, **55**, 511–518.
36 N. Sahiner and A. O. Yasar, *Int. J. Hydrogen Energy*, 2014, **39**, 10476–10484.
37 F. Seven and N. Sahiner, *J. Power Sources*, 2014, **272**, 128–136.
38 N. Sahiner and S. Demirci, *Eur. Polym. J.*, 2016, **76**, 156–169.
39 N. Sahiner, A. O. Yasar and N. Aktas, *Int. J. Hydrogen Energy*, 2016, **41**, 20562–20572.
40 S. Yildiz, N. Aktas and N. Sahiner, *Int. J. Hydrogen Energy*, 2014, **39**, 14690–14700.
41 S. B. Khan, F. Ali and A. M. Asiri, *Int. J. Hydrogen Energy*, 2020, **45**, 1532–1540.
42 H. Naeem, M. Ajmal, S. Z. Khan, M. N. Ashiq and M. Siddiq, *Soft Mater.*, 2021, **19**, 480–494.
43 S. Demirci, K. Sel and N. Sahiner, *Sep. Purif. Technol.*, 2015, **155**, 66–74.
44 N. Sahiner and S. Demirci, *Asia-Pac. J. Chem. Eng.*, 2019, **14**, e2305.
45 M. Arif, M. Shahid, A. Irfan, J. Nisar, W. Wu, Z. H. Farooqi and R. Begum, *RSC Adv.*, 2022, **12**, 5105–5117.
46 M. Farooq, J. Ihsan, S. Saeed, A. Haleem and M. Siddiq, *J. Inorg. Organomet. Polym. Mater.*, 2021, **315**(31), 2030–2042.
47 M. Ajmal, M. Siddiq, H. Al-Lohedan and N. Sahiner, *RSC Adv.*, 2014, **4**, 59562–59570.
48 F. Bibi, M. Ajmal, F. Naseer, Z. H. Farooqi and M. Siddiq, *Int. J. Environ. Sci. Technol.*, 2017, **15**, 863–874.